

Nonisothermal Curing Kinetics of a Novel Polymer Containing Phenylsilylene and Propargyl-Hexafluorobisphenol A Units

Guang Yang, Zehong Yuan, Zhiyong Yang, Maning Zhang

Key Laboratory of Aerospace Materials and Performance (Ministry of Education), School of Materials Science and Engineering, Beihang University, Beijing 100191, China

Correspondence to: G. Yang (E-mail: yangguang@buaa.edu.cn)

ABSTRACT: A novel thermosetting polymer, poly[(phenylsilylene) propargyl-hexafluorobisphenol A] (PBAFS), with a new structure was synthesized. The structure of PBAFS and its cured resins were characterized by Fourier transform infrared spectra. During curing, a hydrosilylation reaction may occur between Si—H and C≡C bonds and a Claisen rearrangement reaction of aryl propargyl ether led to formation of chromene, which immediately preceded polymerization on heating. The dynamic viscosity behavior was investigated by rheological experiment. Thermal stability of the cured PBAFS was also measured by Thermogravimetric analysis. The curing behavior of PBAFS was monitored by nonisothermal differential scanning calorimetry at different heating rates. The kinetic parameters and the kinetic model of the cure reaction were evaluated by Kissinger, Ozawa, and Friedman methods. The cure reaction of PBAFS was found *n*th-order in nature and the prediction curves by Friedman method for nonisothermal curing reaction were in good agreement with the experimental curves. The isothermal curing time of PBAFS were predicted by Vyazovkin and model-fitting methods from the nonisothermal kinetic parameters. © 2012 Wiley Periodicals, Inc. *J. Appl. Polym. Sci.* 000: 000–000, 2012

KEYWORDS: phenylsilylene; propargyl; curing of polymer; kinetics; differential scanning calorimetry (DSC)

Received 14 September 2011; accepted 16 March 2012; published online

DOI: 10.1002/app.37717

INTRODUCTION

A lot of attention has been paid to the polymers which contain silicon or alkynyl structure in main chain because of their excellent heat resistance after curing.^{1–11} In general, the high temperature-resistant polymer mostly contains rigid molecular structure which could improve the heat-resistant but decrease the processing properties simultaneously^{12–14} such as polyimide and polybenzothiazole. Itoh et al.¹⁰ found that poly[(phenylsilylene) ethynylene-1, 3-phenylene-ethynylene], [—Si (Ph) H—C≡C—C₆H₄—C≡C—] (MSP), which contained Si (R) H- structure in the main chain had extremely high thermal stability and had better solubility than many kinds of polyimides, however, the cost of the acetylene terminated polymers was high. Dirlikov,¹⁵ Dirlikov and Feng,¹⁶ and Vinayagamoorthi¹⁷ had reported the propargyl-terminated resins possessing good thermal stability, excellent physico-mechanical properties and low cost. Researchers in our laboratory have focused on the molecular design and synthesis of novel polymers with -Si (R) H- and propargyl groups in the main chain to resolve the conflict between the heat resistance and processing properties. This new structure polymer showed both high temperature resistance and good processability.^{18,19} These unique performances could permit the polymer to be

used as matrix for high-performance composites, such as a potential substitute for polyimides in preparing fiber-reinforced materials.

Although the solubility, processability, and thermal stability of the polymers containing both silylene and propargyl groups have been studied,¹⁹ there is little information about the curing kinetics of the polymers. The curing kinetic characteristics of the thermosets are fundamental to understanding structure-property-processing relationships for the manufacture and utilization of high-performance composites.²⁰ To establish the theoretical basis for design, control, and optimize the curing process, in this article, a novel polymer, poly[(phenylsilylene) propargyl-hexafluorobisphenol A] (PBAFS), was synthesized and its curing kinetics was investigated by nonisothermal differential scanning calorimetry (DSC) at different heating rates.

EXPERIMENTAL

Materials

Lithium aluminum hydride (LiAlH₄) and di-ethylene glycol dimethyl ether (DGDE) (A. R., Tianjin fine chemicals institute China), dipropargyl ethers of hexafluoro-bisphenol A (DPBPF),^{16,21} and phenylsilylene (PhSiH₃)²² (synthesized by

ourselves). Phenylsilylene and DGDE were distilled and dried over 3A molecular sieves prior to use.

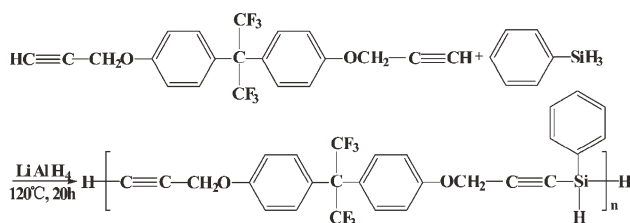
Instrumentation and Characterization

Fourier transform infrared (FTIR) spectra, used to identify the structures of PBAFS and the cured products, were obtained from Nicolet-Avatar 360 spectrometer over the wave-number range 400–4000 cm^{-1} . All samples were prepared as KBr pellets. $^1\text{H-NMR}$ spectra were recorded on a JEOL-AL 300 with CDCl_3 as solvent and tetramethylsilane as the internal standard. Polymer molecular weights were obtained by gel permeation chromatography in tetrahydrofuran (flow rate 1 mL/min) using a Waters 515-2410 System chromatograph analysis apparatus calibrated with polystyrene standard. Thermogravimetric analysis (TGA) was performed in nitrogen at a heating rate of $20^\circ\text{C}/\text{min}$ on a NETZSCH instrument DSC/TGASTA 449C Jupiter. Rheological measurement was carried on Bohlin model Gemini 200 Rheometer with a shear rate of 0.1 s^{-1} at the heating rate of $5^\circ\text{C}/\text{min}$. Curing studies were performed on a Mettler Toledo DSC1 at different heating rates (2, 5, 10, and $15^\circ\text{C}/\text{min}$) over the temperature range from 25 to 400°C under a nitrogen following atmosphere.

Synthesis of PBAFS

The new structure polymer PBAFS was prepared by dehydrogenative coupling polymerization reaction between PhSiH_3 and DPBPF in the presence of LiAlH_4 .¹⁵ The synthesis route is shown in Scheme 1. A 500-mL three-necked flask equipped with reflux condenser, mechanical stirrer bar and nitrogen protection was charged with a mixture of DPBPF (160.78 g, 0.39 mol), LiAlH_4 (0.78 g, 0.02 mol), and DGDE (156 mL) at room temperature. Then PhSiH_3 (44.62 g, 0.41 mol) was added to the flask over a period of 30 min with stirring. The reaction system was further reacted with reflux, stirring and N_2 protection at 120°C for 20 h in an oil bath. The reaction system was cooled to room temperature, then poured into 1N hydrochloric acid (HCl) and extracted with toluene. The organic layer was separated, dried over anhydrous sodium sulfate, and the solvent was removed by rotary evaporation to afford a brown viscous liquid. The viscous liquid was further dried in a vacuum oven at 60°C for 48 h to give a viscous polymer. Yield: 132.0 g, 77.4%. M_w : 35,629.

FTIR (KBr, cm^{-1}): 3299 ($\equiv\text{CH}$ stretching vibration), 2145 (Si-H and $\text{C}\equiv\text{C}$ stretching vibrations), 1173 (CF_3 stretching vibration), 1252 (Ar-O-C stretching vibration). $^1\text{H-NMR}$ (300 MHz, CDCl_3 , ppm): 5.28 (*d*, Si-H), 4.89 (*d*, SiH_2), 2.54 (*d*, $\equiv\text{C-H}$), 4.62 (*m*, CH_2), 6.78–7.58 (*m*, Ar-H).



Scheme 1. Synthesis of PBAFS.

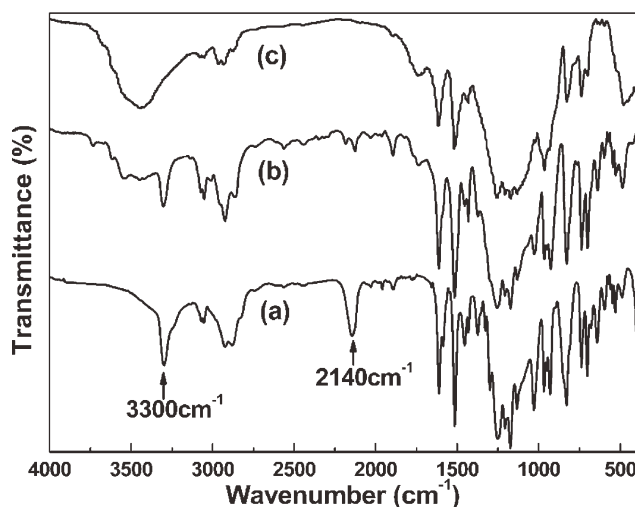


Figure 1. The FTIR spectra of PBAFS and its cured products following the cure process. (a) Uncured resin, (b) cured after $200^\circ\text{C}/4 \text{ h}$, (c) cured after $190^\circ\text{C}/1 \text{ h} + 210^\circ\text{C}/2 \text{ h} + 250^\circ\text{C}/4 \text{ h} + 300^\circ\text{C}/3 \text{ h}$ (10 h total).

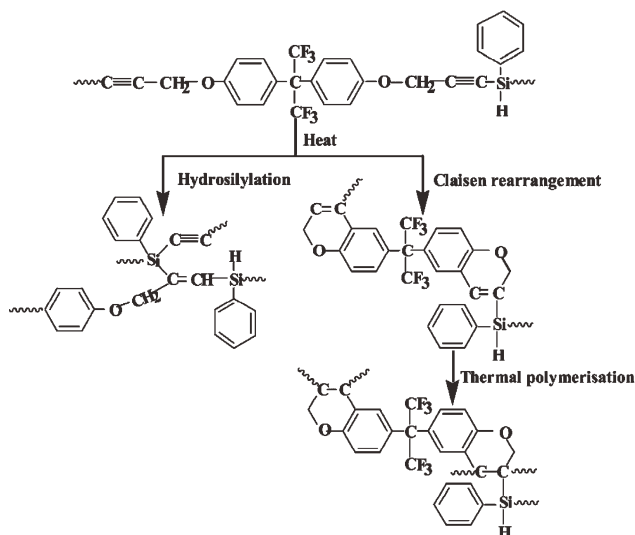
RESULTS AND DISCUSSION

Curing Mechanism of PBAFS

The reaction route for synthesis of PBAFS is shown in Scheme 1. Figure 1 shows the FTIR spectra of uncured PBAFS, cured resins after $200^\circ\text{C}/4 \text{ h}$, and $190^\circ\text{C}/1 \text{ h} + 210^\circ\text{C}/2 \text{ h} + 250^\circ\text{C}/4 \text{ h} + 300^\circ\text{C}/3 \text{ h}$ in an air oven. It was seen that the infrared absorption bands characteristic of $\equiv\text{C-H}$ at 3299 cm^{-1} and of $\text{C}\equiv\text{C}$ and Si-H at 2145 cm^{-1} were decreased remarkably in the curing process. These facts indicated an addition crosslinking reaction that is the hydrosilylation reaction between the Si-H and $\text{C}\equiv\text{C}$ bond, which was reported in the literature of a polymer containing both Si-H and $\text{C}\equiv\text{C}$ bonds.^{23,24} Besides, it is well known that phenyl propargyl ether could undergo Claisen type sigmatropic rearrangement to 2H-chromenes (2H-1-benzopyranes) with thermal treatment and the rearrangement is always accompanied by thermal polymerization.^{25–27} Compared with the thermal polymerization, the formation of the chromene is relatively slow reaction, which is predominant and is the rate determining step.²⁷ The reaction mechanism of the monomer, dipropargyl ethers of hexafluoro-bisphenol A (DPBPF), has been well established.^{28,29} During heat treatment, the intramolecular ring (chromene group) is formed through Claisen rearrangement and immediately followed by thermal polymerization of the formed chromene group. The rearrangement and the followed polymerization reactions for PBAFS were both shown in Figure 1(b,c) by no appearance of the band characteristic of the $\nu(\text{C=C})$ vibration of chromene at 1637 cm^{-1} , which is caused by the rapid consumption of the formed chromene group on heating. Thus, the reaction mechanism of PBAFS is proposed and depicted in Scheme 2.

Dynamic Rheological Analysis of PBAFS

The dynamic viscosity behavior of PBAFS is shown in Figure 2. The polymer was a viscous liquid at room temperature with a viscosity of 20.3 Pa s. The viscosity of the polymer was lower than 1 Pa s in the temperature range of $60\text{--}211^\circ\text{C}$. Compared with MSP¹⁰ which also has both Si-H and $\text{C}\equiv\text{C}$ bond, the



Scheme 2. Reaction mechanism of thermal-polymerized PBAFS.

polymer exhibited excellent flow-ability and had a broader processing window over 150°C. This permitted PBAFS to be processed by a variety of techniques such as resin transfer molding, compression molding for fabricating thermosetting composites.

Thermal Stability of the Cured PBAFS

The TGA curve of the cured sample of PBAFS is shown in Figure 3. It was showed that the T_{d5} (temperature of 5% weight loss) was 465°C and the char yield at 900°C was 61.7%. The T_{d5} of the cured PBAFS under argon is 65°C higher than the thermosets of DPBPF monomer¹⁵ with terminated propargyl group and without phenylsilylene group, which indicated the high thermal stability of the polymer.

Curing Behavior of PBAFS

The curing behavior throughout the course of the reaction can be monitored by nonisothermal scan method. The dynamic DSC curves for PBAFS in the range of 25–400°C at the heating rates of 2, 5, 10, 15°C/min are demonstrated in Figure 4. Obviously, a broad exothermic peak associated with the curing and a

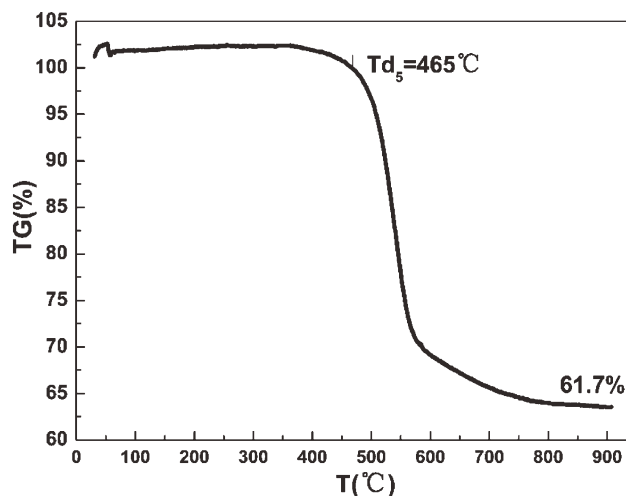


Figure 3. TGA curves for the cured sample of PBAFS.

small one was observed in each dynamic curve. The exothermic peak shifted to the higher temperatures with the increasing heating rate. The first exothermic peak might be attributed to the hydrosilylation reaction and/or Claisen rearrangement which immediately followed by the chromene polymerization. The hydrosilylation reaction involved the Si-H and C≡C bonds might be preceded by the Claisen rearrangement reaction of aryl propargyl ether because each dynamic curve was composed of only one curing exotherm during the curing reaction (shown in Figure 4). The small exotherm at higher temperature might be due to the decomposition of the cured products. Table I shows the characteristic parameters of the curing exothermic peak, T_i (initial temperature in the exotherm), T_{onset} (onset temperature in the exotherm), T_p (peak temperature in the exotherm), and ΔH (exothermic enthalpy under the curing exotherm). It was observed that the peak temperature increased from 259 to 300°C with the increasing heating rate and the onset temperature of curing reaction occurred above 180°C. Compared with the curing behavior of DPBPF ($T_{onset} = 239^\circ\text{C}$, $T_p = 279^\circ\text{C}$, and $\Delta H = 916 \text{ J/g}$ at the heating rate of

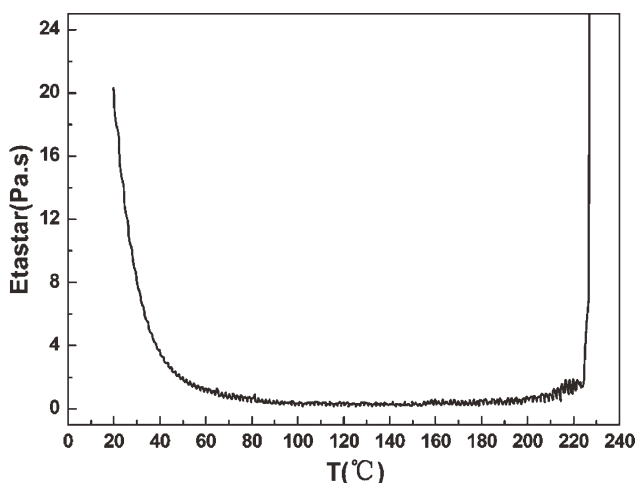


Figure 2. The complex viscosity versus temperature of PBAFS.

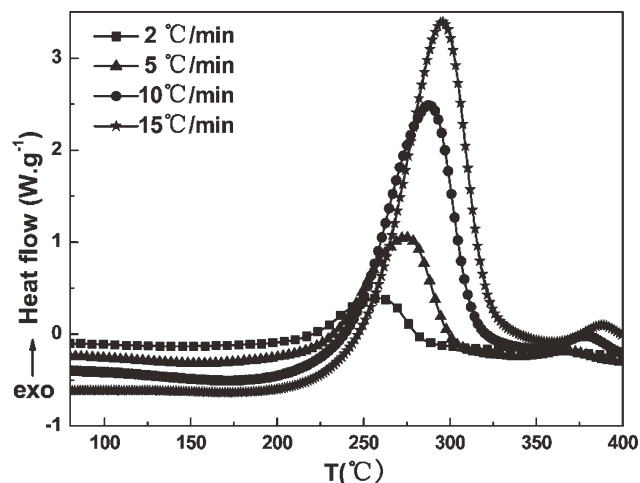


Figure 4. Dynamic DSC curves of PBAFS at different heating rates.

Table I. Characteristic Parameters of the Curing Reaction for PBAFS

Heating rate (°C/min)	T_i (°C)	T_{onset} (°C)	T_p (°C)	ΔH (J/g)
2	185	218	259	749
5	186	230	274	758
10	198	242	287	794
15	209	253	295	661

5°C/min),³⁰ the PBAFS presented lower cure temperature and less exothermic enthalpy, which made it exhibit better processability than DPBPF resin.

Curing Kinetic Analysis

The basic assumption of DSC method is that the measured heat flow (dH/dt) is proportional to the reaction rate ($d\alpha/dt$) and can be calculated by eq. (1):

$$\frac{d\alpha}{dt} = \frac{(dH/dt)}{\Delta H_{total}} \quad (1)$$

where $d\alpha/dt = \beta d\alpha/dT$ at a constant heating rate β , ΔH_{total} is the total reaction heat at a certain heating rate. The degree of conversion (α) is proportional to the heat generated due to cross-linking and can be determined by eq. (2):

$$\alpha_t = \frac{\Delta H_t}{\Delta H_{total}} \quad (2)$$

where ΔH_t is the dynamic reaction heat at time t .

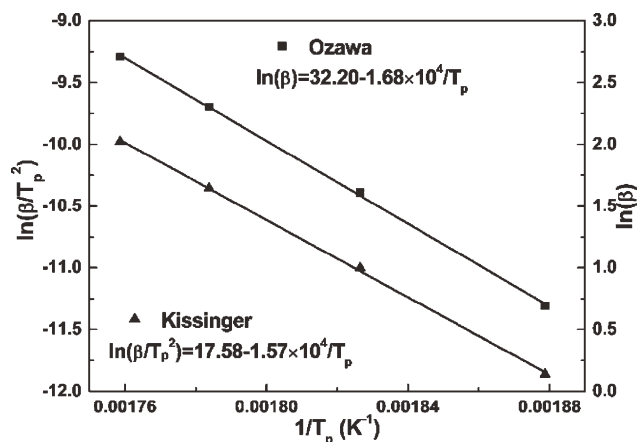
The phenomenological kinetics of cure can be generally described in the differential form as:

$$\frac{d\alpha}{dt} = K(T)f(\alpha) = A \exp\left(\frac{-E_a}{RT}\right)f(\alpha) \quad (3)$$

where $K(T)$ is the Arrhenius rate constant, $f(\alpha)$ is a function determined by the cure mechanism, A and E_a are the Arrhenius parameters (Pre-exponential factor and activation energy, respectively), R is the universal gas constant, and T is the absolute temperature.

The multiple-heating rate of nonisothermal methods such as Kissinger,³¹ Ozawa,³² and Friedman methods,^{33,34} which can quantify the kinetic parameters without requiring prior knowledge of the reaction mechanism, were applied in this article.

The nonisoconversional method of Kissinger and Ozawa assume that the conversion at each DSC exothermic peak is invariant and is independent on the heating rate. Friedman method can determine the activation energy as a function of conversion, which is isoconversional method for application of the data at the same conversion α for a few thermal analysis curves. It assumes that the reaction rate at a constant conversion is only a function of temperature. Compared with the isoconversional method of Flynn–Wall–Ozawa^{35,36} and Kissinger–Akahira–Sunose,^{31,37} Friedman does not introduce any approximations and not restricted to the constant heating rate mode, the activa-

**Figure 5.** Determination of kinetic parameters by Kissinger and Ozawa methods.

tion energy obtained from which is more sensitive to the changes in mechanism.³⁸

Kissinger and Ozawa Methods

According to Kissinger method, E_a is obtained from the maximum reaction rate, where $d(d\alpha/dt)/dt$ is zero at a constant heating rate and the reaction rate is assumed to be maximum at the peak temperature (T_p). The relation equation can be expressed as follows:

$$\ln\left(\frac{\beta}{T_p^2}\right) = \ln\left(\frac{AR}{E_a}\right) - \frac{E_a}{RT_p} \quad (4)$$

where β is the heating rate, and T_p is the peak exothermic temperature at a certain heating rate. Therefore, the values of E_a and A can be obtained from the slope and intercept of the plots of $\ln(\beta/T_p^2)$ versus $1/T_p$, respectively. The plots of $\ln(\beta/T_p^2)$ versus $1/T_p$ are shown in Figure 5. The curing kinetic parameters (E_a and A) were obtained by the values of T_p and β in Table I, which were listed in Table II.

Another method named Ozawa can be also applied to the nonisothermal kinetic analysis. It is based on a linear relationship between the logarithm of heating rate ($\ln \beta$) and the inverse of the exothermic peak temperature ($1/T_p$), eq. (5).

$$\ln(\beta) = \ln\left(\frac{AE_a}{Rf(\alpha)}\right) - 5.331 - 1.052 \frac{E_a}{RT_p} \quad (5)$$

On the assumption of the same degree of conversion at peak temperature for different heating rates, the plots of $\ln \beta$ versus $1/T_p$ should give a straight line with a slope of $1.052E_a/R$. By utilizing Ozawa method, the plots of $\ln \beta$ versus $1/T_p$ are shown

Table II. Kinetic Parameters Obtained by Kissinger and Ozawa Methods for PBAFS

Method	E_a (kJ/mol)	A (min^{-1})
Kissinger method	130.2	6.75×10^{11}
Ozawa method	132.4	-

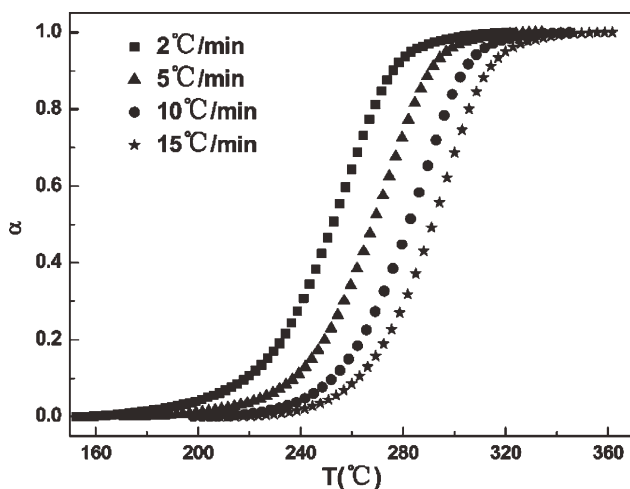


Figure 6. Conversion as a function of cure temperature for PBAFS at different cure rates.

in Figure 5 and the calculated E_a value was listed in Table II. The values of E_a obtained by Kissinger and Ozawa methods were similar with each other, which were 130.2 and 132.4 kJ/mol, respectively.

Friedman Method

Both Kissinger and Ozawa methods can only provide a single activation value for the overall curing process which is obviously not effective to afford information about characteristics of the curing reactions. Therefore, the isoconversional method of Friedman which can provide the activation energy as a function of conversion is more appropriate to be used. For different heating rate, the Friedman method directly evaluates eq. (3) at a specific degree of cure α :

$$\ln \frac{d\alpha}{dt} = \ln[A_2 f(\alpha)] - \frac{E_a}{RT_\alpha} \quad (6)$$

For a certain α , the first term on the right side of eq. (6) is a constant and the pairs of $(d\alpha/dt)_\alpha$ and T_α at several heating rates can be derived from the measured DSC curves. Figure 6 shows the degree of conversion as a function of temperature at various heating rates. From the slope of the plots of $\ln (d\alpha/dt)_\alpha$ versus $1/T_\alpha$ (shown in Figure 7), the activation energy values at each conversion can be obtained. As is shown in Figure 8, the value of E_a increased from 120.5 to 144.9 kJ/mol with the increasing degree of conversion from 0.1 to 0.9 and the average value for the whole range was 133.8 kJ/mol. One interpretation of this behavior is an apparent decrease in molecular mobility during the curing process.³⁹ Another interpretation is that the kinetic process may involve parallel reactions or reactions occurring simultaneously.^{40,41} As shown in Figure 4, only a single curing exotherm was observed in DSC profits of PBAFS, it implied that the hydrosilylation reaction and Claisen rearrangement reaction are almost occurred at the same temperature range. The kinetics of the former can be expected to be in tune with that of the latter reaction and can be studied indirectly from the DSC themogram.

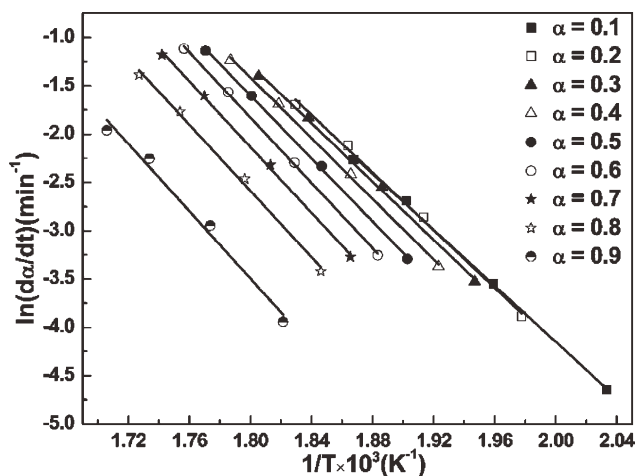


Figure 7. Isoconversional plots for $\ln (d\alpha/dt)_\alpha$ versus $1/T_\alpha$.

Curing Kinetic Model

For the cure of thermosetting systems, the general method taken is to treat kinetic analysis as phenomenological in nature, which ignores the complexity of cure in kinetic calculations.⁴⁰ To examine kinetic model, the value of the activation energy should be estimated previously. In this article, the average E_a value determined by Ozawa method was applied. In general, the mechanisms of thermosets curing are classified into two major kinetic reactions, an n th-order and autocatalytic reactions.⁴² In case of n th-order reaction, the Friedman method based on eq. (7) can be applied to find the kinetic model.^{20,43}

$$\ln[Af(\alpha)] = \ln \frac{d\alpha}{dt} + \frac{E_a}{RT} = \ln A + n \ln(1 - \alpha) \quad (7)$$

The value of $\ln [Af(\alpha)]$ can be derived by values of $\ln [d\alpha/dt]$ and E_a/RT from measured DSC curves. If the curing reaction follows n th-order model, a straight line would be yielded by plotting $\ln [Af(\alpha)]$ versus $\ln(1 - \alpha)$ and the maximum reaction rate occurs at the beginning of the reaction ($\alpha = 0$).⁴⁴ The slope and intercept of the straight line are correspond to the reaction

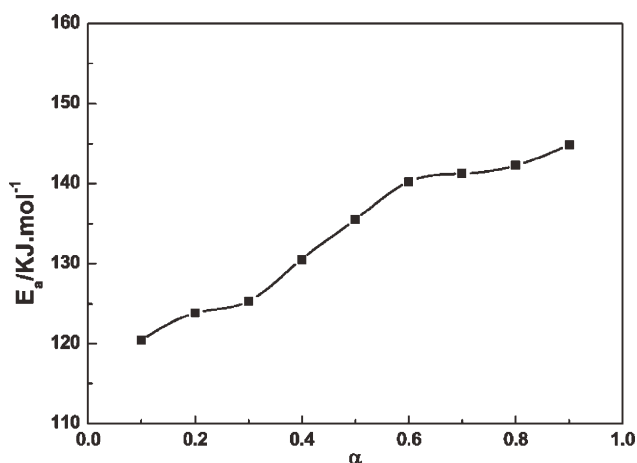


Figure 8. Variation of E_a versus conversion α for PBAFS.

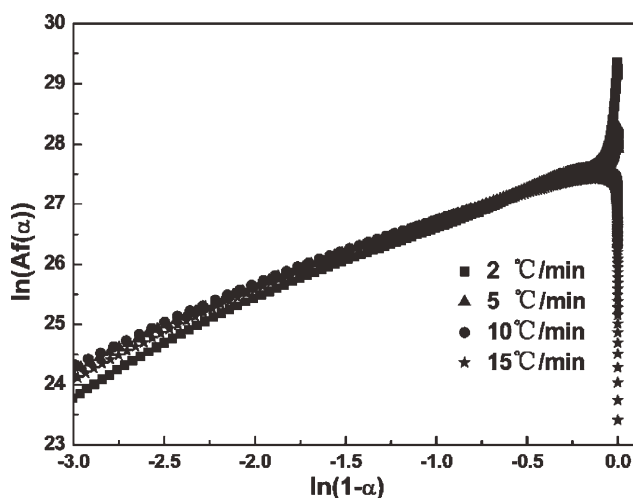


Figure 9. Plots of $\ln [Af(\alpha)]$ versus $\ln (1 - \alpha)$ for PBAFS at different heating rates.

order n and $\ln A$, respectively. However, as for autocatalytic process, the plots would show a maximum of $\ln (1 - \alpha)$ at the degree of conversion around 0.2 to 0.4 [$\ln (1 - \alpha)$ around -0.51 to -0.22], which reflects the nature of the autocatalytic reaction.^{20,45}

Figure 9 shows the plots of $\ln [Af(\alpha)]$ and $\ln (1 - \alpha)$ at different heating rates. Because $\ln [Af(\alpha)]$ and $\ln (1 - \alpha)$ shows a maximum at the beginning of the reaction closed to $\alpha = 0$ and displays good linear relationship except the very beginning, this suggests that curing reaction of PBAFS is n th-order in nature. Because of the n th-order character of PBAFS, the n th-order kinetic model may give a better description of the nonisothermal reactions considered here and the reaction rate can be expressed as follows:

$$\frac{d\alpha}{dt} = A \exp\left(-\frac{E_a}{RT}\right)(1 - \alpha)^n \quad (8)$$

Model Fitting and Comparison

According to eq. (7), the pre-exponential factor A and the reaction order n can be obtained by linear regression method. The straight line part was applied to fit the kinetic parameters and the evaluated values were summarized in Table III. The

Table III. Kinetic Parameters Evaluated for Nonisothermal Curing Reaction

Heating rate (°C min ⁻¹)	E_a^a (kJ mol ⁻¹)	n	A ($\times 10^{12}$ min ⁻¹)	
			Mean	Mean
2	132.4	1.28	1.17	1.28×10^{12}
5		1.15		1.26
10		1.10		1.20
15		1.16		1.20

^aObtained by Ozawa method.

pre-exponential factor A varied from 1.28×10^{12} to 1.2×10^{12} min⁻¹ with the increasing heating rate. There was no significant effect of heating rate on the pre-exponential factor and the reaction order for the curing reaction. The average values of n and A were 1.17 and 1.24×10^{12} min⁻¹, respectively. To verify the accuracy of the established kinetic model, the experimental data and the predicted curves based on the determined kinetic parameters for curing reaction of PBAFS at different heating rates are compared in Figure 10. It is obviously that the predicted curves are in good agreement with the experimental results throughout most of the temperature range for PBAFS. However, the slight deviations were observed at higher conversion. As we know, in the later stages of the thermosetting resins curing, the mobility of functional groups may have been hindered so that the rate of the curing would be controlled by diffusion rather than chemical factors. This may be the reason why there are slightly deviations in the later stage of the cure. Besides, the predicted curves progressively shift to lower temperatures as the increasing heating rate (especially at the heating rate of 15°C min⁻¹). It may be attributed to the thermal lag in dynamic curing process and the effect becomes more obvious with the increasing heating rate.

Isothermal Curing Time Prediction

Prediction of conversion dependency on the curing time under isothermal condition is useful in practical applications for evaluating isothermal behavior of thermosets from nonisothermal experiment data. The reliability of the predictions depends on an approach used to define the kinetic triplets (the activation energy, the pre-exponential factor, and the reaction model).⁴⁶

According to Vyazovkin method,^{47,48} an integrated eq. (9) from eq. (3) can be used to predict the isothermal curing time at a certain temperature T_0 .

$$t_x = \frac{\frac{1}{\beta} \int_0^{T_x} \exp(-E_a/RT) dT}{\exp(-E_a/RT_0)} \quad (9)$$

where t_x is the time to reach the degree of conversion α at a certain temperatures under isothermal conditions. By this method, the dependence of E_a on α (obtained by Friedman method) and experimental values of T_x can be applied to calculated the dependence of α on t under isothermal conditions.

According to eq. (8), the equation relating time, temperature, and conversion is given as:

$$\alpha = 1 - [1 - (1 - n)At \exp(-\frac{E_a}{RT})]^{(\frac{1}{1-n})} \quad (10)$$

Take the nonisothermal kinetic parameters of Table III into eq. (10), equation relating the time and α can be obtain as eq. (11) which was called "Model-fitting method".

$$t_x = \frac{(1 - \alpha)^{-0.17} - 1}{2.11 \times 10^{11} \exp(-\frac{1.59 \times 10^4}{T})} \quad (11)$$

The time-conversion curves predicted for the isothermal cure of PBAFS at 240°C by Vyazovkin and model-fitting methods are

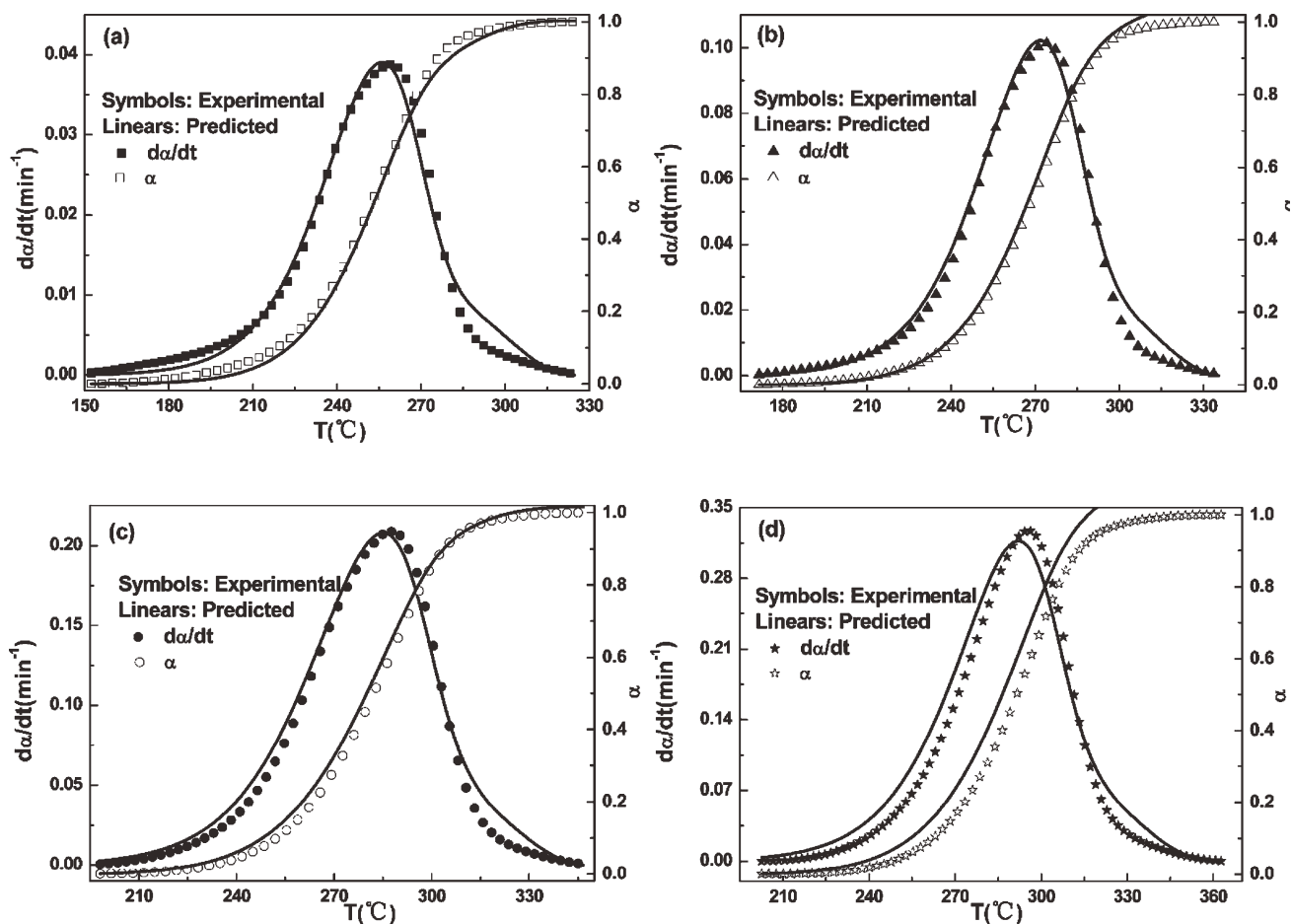


Figure 10. Comparisons of the predictions, dependence of $d\alpha/dt$ and α on temperature, with the experimental curves for PBAFS at different heating rates: (a) 2°C/min, (b) 5°C/min, (c) 10°C/min and (d) 15°C/min.

compared with the experiment values and shown in Figure 11. It showed that the predicted curves by the two methods were both closed to experimental data, especially the prediction by model-fitting method. A close match between the experiment data with predicted values showed the validity of the calculated kinetic parameters. However, it is also worthy of note that, the model-fitting method has not detected the complex nature of the studied cure kinetics.

CONCLUSIONS

A novel polymer poly [(phenylsilylene) propargyl-hexafluorobisphenol A] (PBAFS) was prepared by dehydrogenative coupling polymerization reaction. The kinetic process of PBAFS involved hydrosilylation reaction between Si-H and $C\equiv C$ bonds and the Claisen rearrangement of the phenyl propargyl ether group leading to form the intermediate chromene which consumed immediately on heating. The polymer displayed excellent flow-ability and high thermal stability by the analysis of the dynamic viscosity and TGA curves. The curing behavior monitored by nonisothermal DSC method showed a single curing exothermic peak with T_p in the range of 260°C–295°C depending on the heating rate and the onset temperature of polymerization occurred

above 210°C. The values of E_a calculated by Kissinger and Ozawa methods were similar, which were 130.2 and 132.4 kJ/mol, respectively. The cure reaction of PBAFS was found n th-

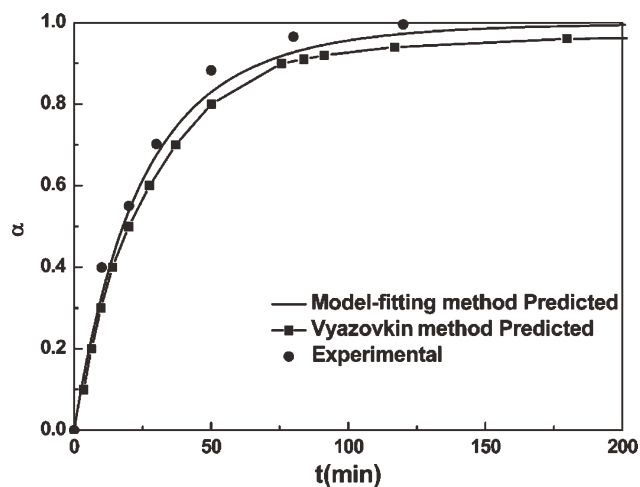


Figure 11. The predicted conversion-time curves and experimental data at 240°C for PBAFS.

order in nature. The reaction order n and A were 1.17 and $1.24 \times 10^{12} \text{ min}^{-1}$, respectively. The prediction of the conversion advancement with temperature was in good agreement with the experiment data. In addition, the isothermal curing time at 240°C predicted by Vyazovkin and model-fitting methods from the kinetic parameters were close to the experimental plots.

REFERENCES

- Itoh, M.; Mitsuzuka, M.; Iwata, K.; Inoue, K. *Macromolecules* **1994**, *27*, 7917.
- Ogasawara, T.; Ishikawa, T. *J. Compos. Mater.* **2002**, *36*, 143.
- Agag, T.; Takeichi, T. *Macromolecules* **2003**, *36*, 6010.
- Wang, M. C.; Wei, L. H.; Zhao, T. *J. Appl. Polym. Sci.* **2006**, *99*, 1010.
- Li, Q.; Zhou, Y.; Hang, X. D.; Deng, S. F.; Huang, F. R.; Du, L.; Li, Z. P. *Eur. Polym. J.* **2008**, *44*, 2538.
- Huang, J. X.; Du, W.; Zhang, J.; Huang, F. R.; Du, L. *Polym. Bull.* **2009**, *62*, 127.
- Vinayagamoorathi, S.; Chinnaswamy, T. V.; Alam, S.; Nanjundan, S. *Eur. Polym. J.* **2009**, *45*, 1217.
- Zhang, L. L.; Gao, F.; Wang, C. F.; Zhang, J.; Huang, F. R.; Du, L. *Chin. J. Polym. Sci.* **2010**, *28*, 199.
- Kimura, K.; Nishichi, A.; Yamashita, Y. *Polym. Adv. Technol.* **2004**, *15*, 313.
- Itoh, M.; Inoue, K.; Iwata, K.; Mitsuzuka, M.; Kakigano, T. *Macromolecules* **1997**, *30*, 694.
- Itoh, M.; Inoue, K.; Iwata, K.; Ishikawa, J.; Takenaka, Y. *Adv. Mater.* **1997**, *9*, 1187.
- Simone, C. D.; Scola, D. A. *Macromolecules* **2003**, *36*, 6780.
- Ghosh, N. N.; Kiskan, B.; Yagci, Y. *Prog. Polym. Sci.* **2007**, *32*, 1344.
- Yagci, Y.; Kiskan, B.; Ghosh, N. N. *J. Polym. Sci. Part A: Polym. Chem.* **2009**, *47*, 5565.
- Dirlikov, S. *Chem. Tech.* **1993**, *10*, 32.
- Dirlikov, S.; Feng, Y. *Polym. Prepr.* **1990**, *31*, 322.
- Vinayagamoorathi, S.; Vijayakumar, C. T.; Alam, S.; Nanjundan S. *Eur. Polym. J.* **2009**, *45*, 1217.
- Yang, G.; Zhang, M. N. China Pat. **2008**, CN101381463B.
- Yang, G.; Zhang, M. N. Int Conf Adv Mater Dev Perform, Beijing, **2008**, 207.
- Lu, Y. B.; Li, M. M.; Ke, L. L.; Hu, D.; Xu, W. J. *J. Appl. Polym. Sci.* **2011**, *121*, 2481.
- Inbasekaran, M. N.; Dirlikov, S. K. U.S. Pat. **1989**, 4,885,403.
- Itoh, M.; Inoue, K.; Ishikawa, J.; Iwata, K. *J. Organomet. Chem.* **2001**, *629*.
- Itoh, M.; Inoue, K.; Iwata, K.; Ishikawa, J.; Takenaka, Y. *Adv. Mater.* **1997**, *9*, 1187.
- Itoh, M.; Iwata, K.; Ishikawa, J.-I.; Sukawa, H.; Kimura, H.; Okita, K. *J. Polym. Sci. Part A: Polym. Chem.* **2001**, *39*, 2658.
- Douglas, W. E.; Overend, A. S. *Eur. Polym. J.* **1991**, *27*, 1279.
- Prieto, S.; Galia, M.; Cadiz, V. *Macromol. Chem. Phys.* **1998**, *199*, 1291.
- Reghunadhan Nair, C. P.; Bindu, R. L.; Krishnan, K.; Ninan, K. N. *Eur. Polym. J.* **1999**, *35*, 235.
- Grenier, M. F.; Sanglar, C. *High Perform. Polym.* **1996**, *8*, 341.
- Grenier, M. F.; Sanglar, C. *High. Perform. Polym.* **1996**, *8*, 315.
- Richer, S.; Alamertery, S.; Paisse, O.; Raffin, G.; Sanglar, C.; Waton, H.; Grenier-Loustalot, M. F. *Polym. Polym. Compos.* **2001**, *9*, 81.
- Kissinger, H. E. *Anal. Chem.* **1957**, *29*, 1702.
- Ozawa, T. *J. Therm. Anal.* **1970**, *2*, 301.
- Vyazovkin, S.; Lesnikovich, A. *Thermochim. Acta.* **1992**, *203*, 177.
- Salla, J. M.; Fernández-Francos, X.; Ramis, X.; Mas, C.; Mantecón, A.; Serra, A. J. *Therm. Anal. Calorim.* **2008**, *2*, 385.
- Ozawa, T. *Bull. Chem. Soc. Jpn.* **1965**, *38*, 1881.
- Flynn, J. H.; Wall, L. A. *J. Polym. Sci. Part B: Polym. Lett.* **1966**, *4*, 323.
- Ozawa, T. *Thermochim. Acta.* **1992**, *203*, 159.
- Gabilondo, N.; López, M.; Ramos, J. A.; Echeverría, J. M.; Mondragon, I. J. *Therm. Anal. Cal.* **2007**, *90*, 229.
- Jubsilp, C.; Punson, K.; Takeichi, T.; Rimdusit, S. *Polym. Degrad. Stab.* **2010**, *95*, 918.
- He, G.; Riedl, B.; Ait-kadi, A. *J. Appl. Polym. Sci.* **2003**, *87*, 433.
- Vyazovkin, S.; Lesnikovich, A. *Thermochim. Acta* **1990**, *165*, 273.
- Yang, G. Z.; Wu, M.; Lu, S.; Wang, M.; Liu, T. X.; Huang, W. *Polymer* **2006**, *47*, 4816.
- Friedman, H. L. *J. Polym. Sci. Part C: Polym. Symp.* **1964**, *6*, 183.
- Prime, B. In Thermal Characterization of Polymeric Materials; Turi, E. A. Ed.; Academic Press: New York, **1981**.
- Yousefi, A.; Lafleur, P. G.; Gauvin, R. *Polym. Compos.* **1997**, *18*, 157.
- Vyazovkin, S.; Linert, W. *Anal. Chim. Acta.* **1994**, *295*, 101.
- Vyazovkin, S.; Sbirrazuoli, N. *Macromol. Rapid Commun.* **2006**, *27*, 1515.
- Ghaemy, M.; Barghamadi, M. *J. Appl. Polym. Sci.* **2009**, *112*, 1311.